The influence of Li^+ and H^+ distribution on the crystal structure of $Li_{7-x}H_xLa_3Zr_2O_{12}$ ($0 \leq x \leq 5$) garnets

Alodia Orera*[1], Guillermo Larraz[1], J. Alberto Rodríguez-Velamazán[1,2], Javier Campo[1], María Luisa Sanjuán[1]

[1]Instituto de Ciencia de Materiales de Aragón (ICMA), CSIC - Universidad de Zaragoza, E- 50009 Zaragoza, Spain

[2] Institut Laue-Langevin, 38042 Grenoble Cedex 9, France.

ABSTRACT

With appropriate doping or processing, $Li_7La_3Zr_2O_{12}$ is an excellent candidate to be used in Li batteries either as a solid electrolyte or as a separator between the Li anode and a liquid electrolyte. For both uses the reactivity with water either from the air or in aqueous media is a matter of interest. We address here the structural changes undergone by $Li_7La_3Zr_2O_{12}$ as a result of H^+/Li^+ exchange and relate them with the amount of proton content and atomic distribution. Neutron diffraction is performed to elucidate lithium and proton location. Two different cubic phases derive from $Li_7La_3Zr_2O_{12}$ through H^+/Li^+ exchange: Deep hydration up to 150 °C yields a non centrosymmetric $I\bar{4}3d$ phase in which octahedral lithium ions are exchanged by protons, tetrahedral lithium ions split into two sites with very different occupancies and protons form O_4H_4 entities around the less occupied tetrahedral site. Annealing above 300 °C results in a centrosymmetric $Ia\bar{3}d$ phase with lower proton content in which Li ions occupy the usual sites of the cubic garnets and protons occupy a split pseudooctahedral site. The centrosymmetric or non centrosymmetric character is determined by the temperature at which exchange is performed and the proton content. Both factors are not independent: at low temperature the high proton content favors proton ordering around the vacant tetrahedra while low proton content and higher mobility at 350 °C lead to a disordered configuration of Li and H ions. The deeply hydrated garnets are stable up to at least 300 °C and also upon ageing at RT.

INTRODUCTION

In the last ten years, $Li_xA_3M_2O_{12}$ compounds with garnet-type structure have been intensively investigated as possible electrolytes in all-solid-state Li batteries (see Refs. 1 and 2 for a description of the structure and a review of properties of these materials). However, their applicability may be compromised by the known reactivity of these materials with H_2O or CO_2, which result in the loss of a non-negligible amount of lithium and also in the appearance of lithium-rich secondary phases that may be detrimental for conductivity. Hydration processes through proton for lithium exchange, in particular, have been reported for several Li-conducting garnets.[3,4,5,6,7,8,9,10] It has to be noted that, though in principle it was assumed that hydration is harmful and has to be avoided, a recent paper on exchanged cubic $Li_7La_3Zr_2O_{12}$ takes advantage of the stability of the most hydrated compound to propose its possible use as a separator between the Li anode and the electrolyte in aqueous Li batteries.[11] A similar proposal[12] has been made for $Li_{5+2x}La_3Ta_{2-x}Y_xO_{12}$. In this context, it is clear that the reactivity and/or stability of these materials in contact with water has to be thoroughly investigated.

$Li_7La_3Zr_2O_{12}$ (LLZO) is one of the members of the family of $Li_xA_3M_2O_{12}$ garnets with the highest lithium content; it presents the particularity of being tetragonal in its most stable form at RT,[13] instead of the usual cubic unit cell of the garnet structure with $Ia\bar{3}d$ space group (sg). The high lithium content of LLZO results in an especially high sensitivity of this compound to moisture. Hydration processes, for instance, were found to induce the transformation of LLZO to a cubic phase at a much lower temperature (100-150 °C) than expected from the phase transition temperature for stoichiometric LLZO (T_c ~640 °C on heating).[8]

We have previously reported that a cubic form of $Li_7La_3Zr_2O_{12}$ can be produced by prolonged annealing in air at temperatures of about 300-350 °C.[8] The X-ray diffraction (XRD) patterns could be satisfactorily explained within the same sg of archetype garnet structure, $Ia\bar{3}d$. Thermal analysis as well as the detection of Li_2CO_3 by Raman scattering suggested that the cubic garnet had been produced by the proton/lithium exchange mechanism resulting in a composition of type $Li_{7-x}H_xLa_3Zr_2O_{12}$.

In a recent work Wang et al.[10] have also addressed the mechanisms of phase change in LLZO in the presence of H_2O and CO_2. Interestingly, they found that annealing at 350 °C in a dry, CO_2 rich atmosphere also drives tetragonal LLZO (t-LLZO) to a cubic phase by lithium extraction, which in that case would be compensated by oxygen vacancies rather than by proton insertion, resulting in a composition of type $Li_{7-x}La_3Zr_2O_{12-x/2}$.

In a subsequent work we also showed that hydration at low temperature or ageing leads to *a different* cubic form of $Li_{7-x}H_xLa_3Zr_2O_{12}$ type, probably with the non-centrosymmetric $I\bar{4}3d$ sg, though the difficulty in obtaining a single phase of the low-temperature hydrated form precluded the unambiguous determination of its sg. [9]

Due to the low sensitivity of XRD to light elements as lithium and hydrogen, the precise location of lithium ions and protons in the cubic phases derived from LLZO could not be elucidated in our previous works. The aim of this paper is to picture the map of hydrated phases derived from LLZO and relate them with the amount of proton content as well as with the lithium and proton distribution. For this purpose we will submit the samples to air or wet environments at different temperatures during different periods of time. Samples aged at RT will be compared with those exchanged in water at 90°C, or annealed in air both at 150 °C as at 350°C.

Structural evolution as a function of the degree of proton insertion and temperature of treatment are followed by XRD and Raman spectroscopy at RT. Neutron powder diffraction (NPD) of selected, end compounds after treatments at 150 and 350 °C have been performed to elucidate lithium and proton location. The achievement of single phases after these particular treatments allowed the corroboration of the sg assignments. Thermal evolution is studied by variable-temperature XRD and Raman spectroscopy, and also by thermal analysis techniques.

Raman scattering, in particular, proves to be exceptionally sensitive to hydration processes in these materials, both in the region of lattice modes as in the region of OH stretching vibrations. There are spectroscopic hints that allow determining the degree of hydration as well as identifying the centrosymmetric (cs) or non-centrosymmetric (ncs) character of hydrated samples much easier than with XRD, which relies in the intensity of very weak extra diffraction peaks. Finally, Raman scattering is sensitive to secondary phases that are difficult to detect by XRD, either because they are present in very small concentrations or because they contain light-weight elements and are thus weakly diffractive.

EXPERIMENTAL SECTION

Samples preparation: initial parent tetragonal $Li_7La_3Zr_2O_{12}$ samples were prepared by solid state synthesis at 980°C from dry Li_2CO_3 (15 w% excess), La_2O_3 (pre-treated at 900°C) and ZrO_2 (all of them minimum 99% pure).[8] In order to obtain the protonated garnets with variable Li content, H^+/Li^+ exchange was carried out in two different ways: treating the powdered sample in water at 90 °C in reflux conditions or by submitting the tetragonal phase to prolonged annealing in air at intermediate (150 °C) or high (300- 350 °C) temperatures. With this second method, secondary phases of lithium hydroxide and lithium carbonate are formed during the

exchange process. Both phases are water soluble and can be washed out by dipping the sample in water for 2 min under stirring.

The crystal structure of the as prepared tetragonal and proton exchanged garnets was characterized by X-ray and neutron powder diffraction techniques (XRD, NPD). Room temperature XRD experiments were carried out on a Rigaku D/max 2500 diffractometer with Cu Kα radiation working at 40 kV and 100 mA. Variable temperature XRD studies were performed in a X'Pert PRO MPD diffractometer with an Anton Paar HTK1200 heating stage working at 45 kV and 40 mA. NPD data of selected pure phase samples were recorded at the Institute Laue-Langevin (Grenoble) on the D2B high-resolution neutron diffractometer with λ = 1.5942 Å. XRD and NPD patterns were analyzed by the Rietveld method using the FullProf software[14] and the crystal structures were represented with VESTA software.[15] Raman dispersion measurements were performed using a DILOR XY spectrometer with a CCD detector and 1.4 cm^{-1} of spectral resolution. Both 496.5 and 514.53 nm lines of an Ar^+ ion laser were used as excitation source, power at the sample surface being ≤25 mW. Scattered light was collected through a X50 microscope objective lens. A Linkam TS1500V stage was used for in-situ thermal treatments.

Thermogravimetric Analysis (TGA) experiments were carried out in a SDT2960 thermobalance, with heating rates of 10 °C/ under air. Chemical composition of the samples was determined by means of ICP-OES, after washing with water to eliminate secondary phases resulting from the exchange process. Al-doping from the crucibles, if present, was below the detection limit of this technique.

RESULTS

For reference purposes we first present in Figures 1a and 1b the XRD pattern and the Raman spectrum of tetragonal $Li_7La_3Zr_2O_{12}$ (t-LLZO) synthesized by solid state reaction. The diffractogram can be indexed assuming a single garnet phase with tetragonal symmetry and $I4_1/acd$ sg and parameters a= 13.119 Å, c=12.666 Å, in agreement with the literature.[13] The Raman spectrum of t-LLZO grown with natural abundance of lithium isotopes is compared with that 100% enriched in ^6Li, so as to ascertain which modes involve lithium vibrations. According to these spectra, lithium modes are confined to the region between 330 and 600 cm^{-1}, isotope shifts varying between 4 and 18 cm^{-1}, so this region can be expected to be particularly sensitive to changes in the lithium distribution. The region below 150 cm^{-1} involves mainly La vibrations whereas all other modes are ascribed to oxygen vibration, in agreement with Raman selection rules. Of particular interest is the high frequency band appearing at 640 cm^{-1} in t-LLZO. This band is attributed to the stretching vibration of the Zr-O bond and thus will be sensitive to variation in the Zr coordination. In the absence of secondary phases no other modes are found above 700 cm^{-1}.

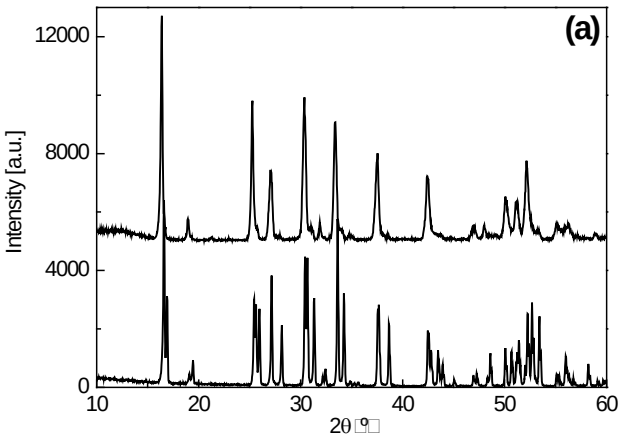

Figure 1a. XRD pattern of a just-prepared tetragonal $Li_7La_3Zr_2O_{12}$ (t-LLZO) sample (lower graph) and of a 3-year aged sample (upper graph).

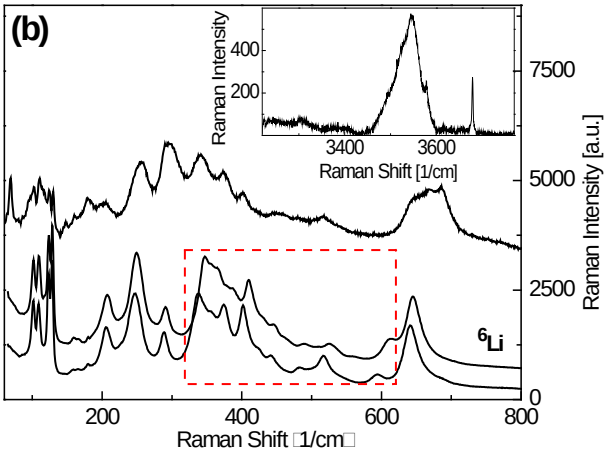

Figure 1b. Effect of ageing on the Raman spectrum of LLZO. The lower graphs pertain to as-prepared t-LLZO produced with natural abundance of lithium isotopes and 100% enriched in the ^{6}Li isotope. The dashed rectangle delimits the region where isotope shifts are found. The upper spectrum belongs to the 3-year old sample whose diffractogram is shown in Figure 1a. The inset shows the region of OH-like stretching vibrations, including peaks from LiOH and LiOH.H_2O at 3675 and 3575 cm^{-1}, respectively.

Ageing at RT

The high sensitivity of LLZO to humidity results, for samples left in contact with air, in an inhomogeneous mixture of phases with varying proton content. In XRD this is seen as a complex diffractogram such as the one shown in Figure 1a, where we present the pattern of a 3-year old sample.

The most intense peaks in the diffractogram of the long-aged sample can be ascribed to a cubic, garnet-like phase with large lattice parameter (a> 13 Å) compared to the average of the tetragonal phase parameters (a= 12.97 Å), which suggests a high degree of hydration. However, even after such a long time small amounts of tetragonal phase remain. The presence of other garnet-like phases cannot be discarded. Due to the complexity of the diffractogram a detailed fit has not been attempted.

Compositional inhomogeneity is also reflected in the Raman spectrum of the aged sample (Figure 1b) which can be interpreted as a superposition of at least two spectra: a weak one belonging to the initial tetragonal phase and another one that we assume belongs to the cubic hydrated phase seen by XRD. Bands arising from Li_2CO_3 are also identified at 100, 157, 195 and 1093 cm^{-1}. The region of O-H stretching vibrations (typically between 3000 and 3800 cm^{-1}, see inset in Figure 1b), presents two types of bands: weak narrow peaks at 3575 and 3675 cm^{-1} are ascribed to LiOH.H_2O and LiOH respectively. The remaining broader features are attributed to stretching vibrations of O-H like entities formed by protons inserted in the garnet phase.

The observation of bands from lithium hydroxides together with OH-like vibrations coming from the garnet confirms that protons have been introduced by the exchange mechanism:

$Li_7La_3Zr_2O_{12} + x\ H_2O \rightarrow Li_{7-x}H_xLa_3Zr_2O_{12} + x\ LiOH$

and not only by a reaction with water of type

$Li_7La_3Zr_2O_{12} + x\ H_2O \rightarrow Li_{7-2x}La_3Zr_2O_{12-x} + 2x\ LiOH,$

suggested in Ref.[16] as a possible mechanism of garnet reaction with water.

The appearance of Li_2CO_3 in the aged sample derives from the partial or total carbonation of LiOH through the reaction $2LiOH + CO_2 \rightarrow Li_2CO_3 + H_2O$. Depending on external conditions such as storage environment, ageing time and thermal treatments, different amounts of lithium hydroxides and/or Li_2CO_3 will appear as secondary phases together with the exchanged garnet. Applying a mild washing procedure serves to eliminate secondary phases such as LiOH, LiOH.H_2O and Li_2CO_3 and allows the sample composition to be analyzed by ICP.

Exchange at T> RT

In the search of obtaining homogeneous samples with a single hydrated phase, t-LLZO samples were submitted to different thermal treatments under a wide range of conditions with temperature varying from 90 to 350 °C and changing the medium between air, vapor or liquid water. From these experiments, we conclude that the optimal experimental conditions to obtain single phases in a reasonable time scale are annealing in air at 150 or at 350 °C.

Annealing in air at 150 °C

The choice of this annealing temperature is based on the observation of a bump in the TG curves of as-grown samples around 150 °C (see Figure S1, curve (a) in the supplementary information). In fact, a 24h treatment of t-LLZO in air at 150°C resulted in a single, cubic garnet phase (c150-LLZO) with the XRD pattern shown in Figure 2. $LiOH.H_2O$ and LiOH by-products were washed out by H_2O without affecting the pattern of the garnet phase. The absence of secondary phases and the homogeneity of the garnet sample allow the chemical analysis of this sample by ICP, resulting in a stoichiometry of $Li_{2.3}H_{4.7}La_3Zr_2O_{12}$, where the proton content has been calculated for charge neutrality. This exchange degree agrees with the proton content calculated from the TGA curve (see Figure S1, curve (b) in supplementary information) which gives an approximate composition of $Li_{2.2}H_{4.8}La_3Zr_2O_{12}$.

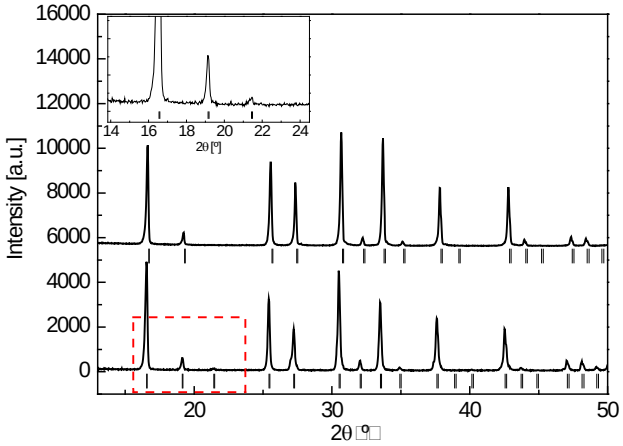

Figure 2. Lower graph: XRD pattern of a LLZO sample (c150-LLZO) annealed in air at 150 °C during 24h. The inset shows a magnification of the low angle region to highlight the peak at 21.4° indexed in the non-centrosymmetric $I\bar{4}3d$ sg. Upper graph: XRD pattern of a LLZO sample annealed in air at 350 °C during several days. Both samples had been washed to remove lithium hydroxides and Li_2CO_3.

The XRD pattern shown in figure 2 can not be fully explained with the $Ia\bar{3}d$ sg usually found for cubic garnets of $Li_xLa_3M_2O_{12}$ type with M a pentavalent or hexavalent cation.[1] This sg, for example, does not explain the weak reflections observed at 2θ= 21.4, 40.2, 53.3 and 64.5°. Previous work by Galven et al. in hydrated $Li_{5+y-x}H_xLa_{3-y}Ca_yNb_2O_{12}$ garnets suggested that intense proton exchange may lead to a non-centrosymmetric phase.[5,6] Two different sg were proposed for different compounds: $I2_13$ and $I\bar{4}3d$. In our case, $I\bar{4}3d$ sg is enough to explain the weak additional peaks. Fitting the XRD pattern of c150-LLZO with this sg gives a large cell parameter (a= 13.087 Å), in agreement with the high exchange level confirmed by ICP analysis. Adopting the ncs $I\bar{4}3d$ structure instead of the cs $Ia\bar{3}d$ one implies important differences in the atomic distribution. Zr atoms, for instance, shift from the centre of the O_6 octahedron, a site which has inversion symmetry and a single Zr-O bond length, toward a (*x*,*x*,*x*) position in $I\bar{4}3d$ implying two different Zr-O bond distances. As regards the available lithium sites, the main difference affects the tetrahedral ones: the single tetrahedral 24*d* site in $Ia\bar{3}d$ splits into two 12*a* and 12*b* sites in $I\bar{4}3d$. Oxygen sites are also split in the ncs structure into two 48*e* sites, compared to the single 96*h* site in $Ia\bar{3}d$.

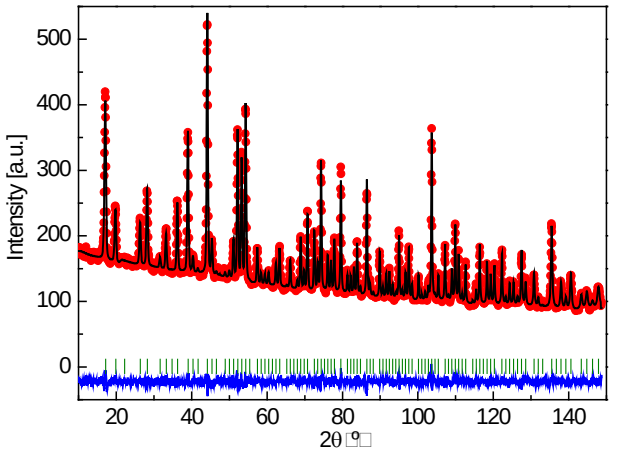

Figure 3. Neutron powder diffractogram of c150-LLZO recorded at 77K. The points are the experimental data and the continuous curve the result of the refinement in the $I\bar{4}3d$ sg with the parameters listed in Tables 1 to 3. The bottom curve represents the difference between the experimental data and the calculated pattern.

Table 1. Refinement results of c150-LLZO NPD data at 77K

Space group	$I\bar{4}3d$ (nº 220)
Unit cell (Å)	a=13.06245 (3)
R_{Bragg}	3.58
R_p (%)	15.4
R_{wp} (%)	12.6
R_{exp} (%)	8.63
χ^2	2.14

Table 2. Refined Structure Parameters (fractional atomic coordinates and occupancies) for c150-LLZO from NPD at 77K

	$I\bar{4}3d$ (nº 220)				
	Site	x	y	z	g
La	24*d*	0.1309(2)	0	0.25	0.99
Zr	16*c*	0.0120(1)	0.0120(1)	0.0120(1)	0.99
Li (1)	12*a*	0.25	0.375	0	0.34
Li (2)	12*b*	0.75	0.625	0	0.908
O (1)	48*e*	0.2862(2)	0.1086(2)	0.1955(2)	1
O (2)	48*e*	0.7273(2)	0.9042(2)	0.8113(2)	1
H	48*e*	0.3441(6)	0.3912(5)	0.0692(6)	0.821

Table 3. Selected Atomic Distances [Å] for c150-LLZO from NPD at 77K

$I\bar{4}3d$ (nº 220)		
La-O(1)	x 2	2.5763
La-O(1)	x 2	2.6134
La-O(2)	x 2	2.5004
La-O(2)	x 2	2.4971
Zr-O(1)	x 3	2.2072
Zr-O(2)	x 3	2.0176
Li(1)-O(1)	x 4	1.9652
Li(2)-O(2)	x 4	1.9986
H-O(1)	x 1	0.9855

A more complete structural analysis was performed using data collected from NPD experiments at 77K, with the main results summarized in Tables 1 to 3. Figure 3 shows the result of the refinement of the NPD data in the aforementioned $I\bar{4}3d$ sg, where a single well-crystallized cubic phase can be observed. As a starting point, and based in our previous NMR results where a preferential exchange of the octahedral Li was observed,[9] a

partial refinement of the structure was performed with a structural model including only La, Zr, O and tetrahedral Li atoms. After this first step, a peak with strong negative scattering density and 48 multiplicity was found in the Difference Fourier map (F_{obs}-F_{calc} Fourier synthesis). Due to the distance of this new 48*e* site to the nearest oxygen atom (~1Å), it was attributed to the presence of incorporated protons, and its coordinates added to the final model. The refinement of this model was very stable with no need of extra constrains, and resulted in a very good agreement with the observed data, with the R-values shown in Table 1. Interestingly, Li ions show a clear preference for the 12*b* tetrahedral site, with occupancy three times higher than that of the 12*a* site. A similar behavior has been reported for other proton exchanged garnet materials in the literature.[5,6] 12*a* and 12*b* sites are ordered such that an octahedral cavity is always sandwiched between a pair of 12*a* and 12*b* sites. As shown in Figure 4, protons are found within the octahedral cages bound to the oxygen atoms (O1) surrounding the less occupied 12*a* Li tetrahedral site, as in $Li_{6-x}H_xCaLa_2Nb_2O_{12}$.[6] In fact, the count of the number of protons (4.9 per unit formula) and vacant 12*a* sites (1 per unit formula) suggests that protons approach preferably *empty* tetrahedra, forming O_4H_4 entities around the lithium vacancy. We note that O_4H_4 units are the most characteristic feature of $A_3Al_2(O_4H_4)_3$ (A= Ca, Sr) hydrogarnets, where *all* tetrahedral sites are empty,[17,18,19] Only one proton position is found in each octahedral cage.

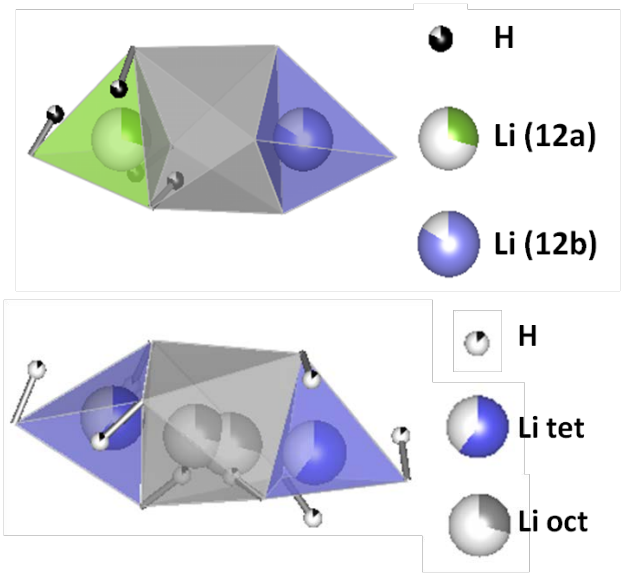

Figure 4. Schematic representation of the lithium and proton sites resulting from the refinement of the NPD patterns of c150-LLZO (top) and c350-LLZO (bottom) within the $I\bar{4}3d$ and $Ia\bar{3}d$ space groups, respectively.

However, it should be noted that the calculated stoichiometry from the refined Li and H occupancies, $Li_{1.9}H_{4.9}$, does not lead to charge neutrality in the chemical formula and differs slightly from that calculated from ICP analysis, $Li_{2.3}H_{4.7}$. A closer look into the residuals in the Difference Fourier synthesis unveils an additional possible site with negative density in the trigonal prismatic cavities of the garnet framework.[1] However, due to the low residual densities all of the refinement attempts with Li or H in this site have resulted in an unstable fit.

Another remarkable aspect is the shift of the Zr atoms from the octahedron center by as much as 0.15 Å, approaching the octahedron face formed by the three O(2) not bonded to protons.

The Raman spectrum of the c150-LLZO sample after washing (see Figure 5, spectrum (a)) is remarkably different from that of t-LLZO shown in Figure 1b, in agreement with the strong structural rearrangement and the absence of a group/subgroup relation between the $I4_1/acd$ and $I\bar{4}3d$ sg.

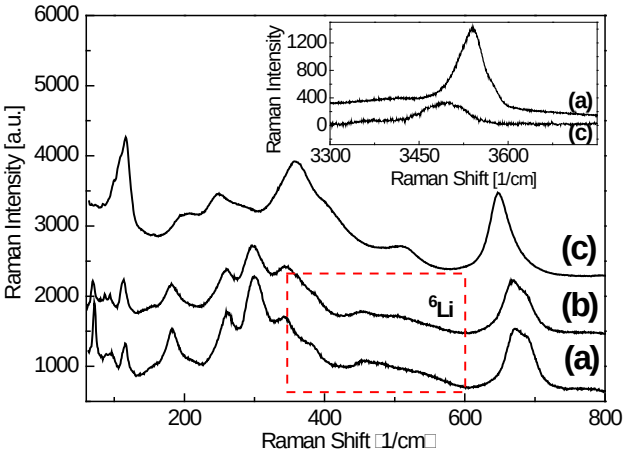

Figure 5. Raman spectra of deeply hydrated c150-LLZO samples produced with natural abundance of lithium isotopes (a), and 100% enriched with 6Li (b). Spectrum (c) belongs to the sample (c350-LLZO). All samples had been washed to remove LiOH and Li_2CO_3. The inset shows the region of OH stretching modes of c150-LLZO and c350-LLZO (after background subtraction).

Regarding the low frequency region of the spectra, the most noticeable features of the c150-LLZO phase are the appearance of an intense narrow band at 70 cm^{-1} and two very intense bands at 260 and 300 cm^{-1} as well as the split aspect of the band above 650 cm^{-1}, ascribed to Zr-O bond stretching. The splitting of the Zr-O band is attributed to the splitting of Zr-O bond distances into two sets in the ncs phase (in the case of t-LLZO, despite the tetragonal symmetry the Zr-O environment is very symmetric with all distances close to 2.11 Å).[13] Remarkable differences are also found in the region of lithium modes. To discuss the lithium activity in this phase the spectrum of a cubic, deeply hydrated sample produced from $^6Li_7La_3Zr_2O_{12}$ is also shown in Figure 5, spectrum (b). As in t-LLZO, isotope effects denoting lithium vibrations are found in some modes between 350 and 600 cm^{-1}. However, compared to t-LLZO, the intensity of Li-related modes is considerably reduced. This is attributed both to the lower lithium content of the exchanged sample as to the change in Raman activity in the ncs phase. We note that, since no occupancy of the octahedral lithium sites has been found, all modes showing isotope shift must involve vibrations of tetrahedral lithium ions.

In the high frequency region of OH^- stretching modes (see inset in Figure 5) a single structureless band with maximum at 3544 cm^{-1} is observed, indicative of a quite simple proton distribution in this sample, in agreement with NPD results. This frequency is slightly lower than those characteristic of basic OH^-, in agreement with the weak hydrogen bond expected from the distance of the proton to the nearest acceptor oxygen atoms (between 2.4 and 2.7Å).

Annealing in air at 300-350°C

In previous works we reported that a cubic form of LLZO with the cs $Ia\bar{3}d$ sg (c350-LLZO) can be produced by exchange in air at 350 °C.[8] Obtaining a homogeneous material requires annealing during several days. Otherwise, as occurs for low-T treatment, a mixture of garnet-like phases with different symmetries and proton content is obtained. The diffractogram of the product after 4 days at 350 °C is shown in Figure 2. Fitting the XRD pattern to $Ia\bar{3}d$ sg gives a= 12.99 Å. According to ICP determination, with annealings at this temperature range proton contents of less than 1.5 protons per formula are obtained. This value is lower than that achieved by annealing treatments at lower temperature, probably due to the simultaneous occurrence of proton for lithium exchange and lithium reinsertion from Li_2CO_3 at 350 ºC, which is close to the main dehydration step (see TG curves in supplementary information).

To elucidate the effect of annealing at 350 ºC on the lithium and proton distribution of LLZO we recorded NPD data of c350-LLZO at 77K. Figure 6 shows the result of the Rietveld refinement of the NPD pattern within the $Ia\bar{3}d$ sg, and Tables 4 to 6 gather the main parameters obtained from the fit. The same procedure as for c150-LLZO was followed: initially, a partial model with La, Zr and tetrahedral Li was tested and then missing atoms were identified from the Difference Fourier synthesis. Two different sites with negative density were found in the octahedral cavities, with distances to the nearest oxygen atom of around 1.9 and 1.1Å, respectively. From these values, these sites were assigned to remaining octahedral Li and inserted H respectively, each of them occupying a split 96*h* site. The Rietveld refinement including these two additional sites yielded a good agreement factor but a still low stoichiometry ($Li_{5.1}H_{1.6}$). To the limit of Fourier map resolution, no octahedral lithium ions were detected at the less-distorted 48*g* octahedral site. This is very likely a consequence of the increase in the tetrahedral site occupancy from one in t-LLZO to almost two ions per formula unit in c350-LLZO.

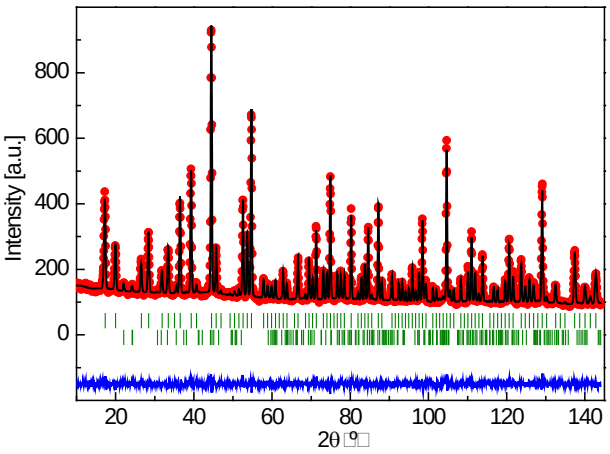

Figure 6. Neutron powder diffractogram of c350-LLZO recorded at 77K. The points are the experimental data and the continuous curve the result of the refinement within the $Ia\bar{3}d$ sg with the parameters listed in Tables 4 to 6. Li_2CO_3 was included in the refinement as second phase. The bottom curve represents the difference between the experimental data and the calculated pattern.

Table 4. Refinement results of c350-LLZO NPD data at 77K

Space group	$Ia\bar{3}d$ (nº 230)
Unit cell (Å)	a=12.97380 (4)
R_{Bragg}	3.86
R_p (%)	14.1
R_{wp} (%)	11.4
R_{exp} (%)	8.41
χ^2	1.86

Table 5. Refined Structure Parameters (fractional atomic coordinates and occupancies) for c350-LLZO from NPD at 77K

$Ia\bar{3}d$ (nº 230)					
	Site	x	y	z	g
La	24*c*	0.125	0	0.25	0.996
Zr	16*a*	0	0	0	1
Li (1)	24*d*	0.375	0	0.25	0.644
Li (2)	96*h*	0.6877(8)	0.5750(8)	0.0991(7)	0.267
O	96*h*	-0.03162(8)	0.0558(1)	0.1493(7)	1
H	96*h*	0.6649(13)	0.6416(12)	0.1055(14)	0.131

Table 6. Selected Atomic Distances [Å] for c350-LLZO from NPD at 77K

$Ia\bar{3}d$ (nº 230)		
La-O	x 4	2.5222
	x 4	2.5719
Zr-O	x 6	2.1077

Li(1)-O	x 4	1.9236
Li(2)-O	x 1	1.8622
	x 1	2.1415
	x 1	2.1458
	x 1	2.2597
	x 1	2.6228
	x 1	2.7317
H-O	x 1	1.0679

The Raman spectrum of c350-LLZO is presented in Figure 5; if we compare it with those of t-LLZO and c150-LLZO we see that the spectrum of c350-LLZO presents broad bands but still resembles the spectrum of t-LLZO whereas no correlation could be established between the spectrum of c150-LLZO and the tetragonal one. The observation of a single band at 650 cm^{-1} in the spectrum of samples annealed above 300 °C is explained by the cs character of the unit cell, with the Zr at the center of the oxygen octahedron and only one Zr-O distance. Regarding the spectrum in the region of O-H stretching vibrations, samples annealed above 300°C present broad features superposed to a strong background whose origin is uncertain but is somehow related to surface phenomena, as it is also observed in other materials where proton insertion on the lattice is not possible. The background is greatly suppressed by the washing procedure, which evidences the presence of an OH-like band at 3494 cm^{-1}. The softening of the OH stretching vibration from 3544 cm^{-1} in c150-LLZO to 3494 cm^{-1} in c350-LLZO agrees with the increase in the bonding distance of the proton from 0.98 to 1.07 Å between both materials.

The resolution of the lithium and proton distributions in c150-LLZO and c350-LLZO samples by NPD throws light about the origin of the structural differences found in proton-exchanged LLZO phases. The main difference arises from the separation of tetrahedral lithium ions into two sites with very different occupancies in the ncs phase, a fact which seems to be connected with the preferential binding of protons to the four oxygen atoms around vacant tetrahedral sites. This in turn requires high proton content. The ordering of the tetrahedral lithium ions as well as that of protons results in the loss of inversion symmetry. On the other hand, the high lithium mobility expected at 350°C and a low proton content are probably at the origin of the cs character of samples annealed at this temperature. The disordered occupation of the tetrahedral sites forces octahedral lithium ions and protons to occupy doubly split sites within the octahedral cavity of the $Ia\bar{3}d$ unit cell, as depicted in Figure 4b.

While the change from the tetragonal to the cs cubic phase is mild and the garnet framework easily accommodates the structural changes, the transformation to the ncs cubic form requires a higher degree of rearrangement. Because of this, the transformation from the tetragonal to the ncs cubic phase apparently is not direct, but needs the formation of at least one intermediate phase. At this respect, it is worth noting that such intermediate phase has not been observed upon exchange of garnets with the conventional $Ia\bar{3}d$ sg, in which proton insertion seems to occur either preserving the $Ia\bar{3}d$ sg (for low proton content) or changing the symmetry to the ncs $I2_13$ cubic sg for the most exchanged cases.[4,5] The evolution through an intermediate phase is clearly observed when t-LLZO samples are left to evolve slowly at RT or are submitted to less efficient proton exchange treatments as follows.

Different experiments at different temperatures and conditions (mainly the exchange media) were performed so as to picture a map of the phases derived from t-LLZO as a function of temperature and the degree of exchange. Exchange at 90 °C in water is presented as an example to highlight the presence of intermediate phases between t-LLZO and ncs cubic LLZO.

Exchange in water at 90 °C

In this set of experiments, t-LLZO was immersed in distilled water and maintained at reflux at 90 °C for different periods up to 26 days. These exchange conditions have been selected due to the high homogeneity of the powder obtained as well as because of the absence of secondary phases, which are soluble in the aqueous exchange media.

The limit composition achieved by this treatment is equivalent to that of the c150-LLZO, close to 2 Li ions per formula, although more than 20 days of treatment were necessary. For shorter periods, neither the

diffractograms nor the Raman spectra shown in Figures S2a and S2b, respectively, indicate single phase content. The diffraction patterns show, with different weight depending on the degree of exposure to water: i) a t-LLZO phase with $I4_1/acd$ sg and lattice parameters similar to those of the as-grown tetragonal garnet, therefore with negligible proton content; ii) an expanded cubic garnet similar to c150-LLZO, and iii) another transient phase that could have tetragonal symmetry but larger unit cell and smaller axiality than the as-grown LLZO. The origin of this novel phase (t'-LLZO), not reported up to now, is still unclear. Its larger unit cell and smaller axiality suggest that it has suffered some Li^+/H^+ exchange but not enough to convert the lattice into cubic symmetry. On the other hand, the broad aspect of the diffraction peaks of both hydrated phases indicates a poor crystallization, especially for the t´ phase.

The nature of this intermediate t´-LLZO phase has been also investigated by means of Raman spectroscopy. The low frequency Raman spectra of samples exchanged in water at 90°C for an increasing number of days (Figure S2b) display an evolution from the spectrum characteristic of the tetragonal garnet to that of a deeply-exchanged cubic garnet analogous to c150-LLZO. For intermediate situations the spectra are, as XRD patterns, quite complex and don't allow and unambiguous identification of a third spectrum that might be attributed to the transient tetragonal phase. However, we may find some hints of peaks belonging to that phase by exclusion of those arising from either the starting tetragonal phase or belonging to the end, cubic hydrated phase. Thus, this phase would be characterized by narrow peaks at 196, 255, 273, 295, 307, 347, 370 and 397 cm^{-1} as well as by a low frequency band at 112 cm^{-1}. The Zr-O band is asymmetric or split, its maximum being around 650 cm^{-1}.

With regard to the high frequency region (3000-3800 cm^{-1}), the most prominent feature is the appearance of an intense band extending from 3450 to 3600 cm^{-1} consisting of up to 4 components at 3495, 3523, 3544 and 3570 cm^{-1}. As the level of hydration is increased the total intensity of the band increases as expected, but a change on the relative intensities of its components is observed, so that the high frequency components gain intensity at the expenses of the low frequency ones until it reaches the aspect observed for c150-LLZO. This trend, together with the evolution of the XRD patterns, according to which the amount of cubic phase increases and that of the t' phase decreases with the treatment duration, lead us to conclude that the components at 3495 and 3523 cm^{-1} belong to the intermediate t' phase and that they arise from proton sites different to those of the limit cubic phase. Additional broad features appear at 3300 and 3380 cm^{-1}. As these bands are not present in either the initial or final garnet phases, they are also attributed to the intermediate phase.

Thermal evolution and stability of hydrated garnet phases

We have so far identified four different phases of garnets related to LLZO: a tetragonal non-hydrated t-LLZO phase with $I4_1/acd$ sg, a cubic non-centrosymmetric (c-ncs) phase of samples deeply hydrated at or below 150 °C ($I\bar{4}3d$ sg), a cubic centrosymmetric (c-cs) phase of samples annealed above 300 °C ($Ia\bar{3}d$ sg) and finally a possibly tetragonal hydrated phase with intermediate proton content (t') that appears for moderate exchange at low temperatures. These phases differ in proton content but also in structural properties such as symmetry and ionic distribution.

In regard with the possible use of LLZO in contact with aqueous electrolytes, the compositional and thermal stability of these hydrated garnets has been investigated. Another interesting point is the possible transformation from one phase to the other. Since the main difference between the cubic ncs and cs phases arises from the distribution and amount of lithium and proton ions, we have searched whether a reversible transformation between cs and ncs phases can occur by varying thermal and hydration conditions. For that purpose, the thermal evolution of selected compositions achieved as single phase has been tested by temperature dependent XRD and Raman scattering.

The thermal evolution of $Li_{7-x}H_xLa_3Zr_2O_{12}$ compounds depends to a great extent on the composition of the starting material and whether the garnet is accompanied by other Li-containing phases, such as hydroxides or carbonates. If Li-containing second phases are absent, the protonated garnet decomposes soon after the dehydration step starting around 350 °C (see Figure S3a in the supplementary information), probably because the structure can not stand the amount of oxygen vacancies required to compensate for proton loss. However, if Li-containing secondary phases are present (either formed during the exchange or provided afterwards), lithium can be reinserted at several stages of the heating run, thus altering the composition and even the symmetry of the garnet. If enough lithium is provided, the garnet recovers the $Li_7La_3Zr_2O_{12}$ stoichiometry and tetragonal symmetry, evidencing the full reversibility of the H^+/Li^+ exchange process.

The temperatures at which lithium reinsertion can occur depend on the nature of the Li-source but also on experimental conditions. Lithium hydroxide, for instance, can react with the exchanged garnet around 220 °C resulting in lithium reinsertion in the garnet together with water loss. However, with enough time in the presence of CO_2 at low temperature, LiOH will end in the form of Li_2CO_3. The stability of this lithium carbonate will depend on its crystallization conditions, and therefore reinsertion of the Li ions in the garnet structure will take place between 400 and 630 °C, leading to the partial recovery of the symmetry and stoichiometry of t-LLZO. At higher temperatures (> 700°C), decomposition of the garnet phase and the consequent appearance of pyrochlore is observed (see Figure S3b in the supplementary information).[8]

Regarding the stability of the specific crystal structures studied throughout this paper, we show in Figure S4 of the supplementary information the XRD pattern of the highly hydrated (and washed) c150-LLZO sample at 300 ºC and after cooling back to RT from 300 °C. It is clearly seen that the $I\bar{4}3d$ sg is maintained and no long range structural changes have taken place in this temperature range. In particular, no transformation to the cs cubic phase is observed, which is attributed to the blocking effect of protons on the lithium mobility. To deepen into this question, the evolution of the Raman spectrum of the c150-LLZO sample as a function of temperature is presented in Figure S5 of the supplementary information. It is clear that even at 300 °C the spectrum still belongs to the $I\bar{4}3d$ ncs phase. The spectral change from 300 to 350 ºC is attributed to a stoichiometry change because of incipient deprotonation. Above 350 °C decomposition results in the appearance of pyrochlore-like bands superposed to the garnet spectrum.

Finally, it is worth noting that conversion of a cs sample to the ncs phase is possible by introducing additional protons into the cs structure at low temperature, for example after long storage periods or low temperature annealings.

DISCUSSION

The diffractometric and spectroscopic results provided above show that the landscape of phases derived from LLZO upon proton insertion is complex and depends not only on the total proton content but also on the dynamic state of protons and lithium ions, which can be altered by varying the temperature at which exchange takes place.

When protons are exchanged at T ≤ 150°C a non-centrosymmetric cubic garnet phase with $I\bar{4}3d$ sg is formed, in which protons are bonded to oxygen anions to form OH-like entities. The transformation from the initial tetragonal $I4_1/acd$ phase toward the ncs cubic phase seems to occur through at least one intermediate phase with probably lower than cubic symmetry (t'). Thus, if hydration is produced just by ageing at RT or if the exchange temperature is below 100°C an inhomogeneous mixture of the ncs cubic and this intermediate t' phase is obtained. Annealing during 24h at 150°C, however, yields a homogenously exchanged garnet of composition $Li_{2.3}H_{4.7}La_3Zr_2O_{12}$ and $I\bar{4}3d$ sg. When exchange is performed at high temperature (≥300°C) lithium mobility and limited exchange yield a cubic centrosymmetric structure with $Ia\bar{3}d$ sg.

Regarding the Li sites, previous reports agree that in stoichiometric t-LLZO lithium ions order in three crystallographic sites (8*a*, 16*f*, 32*g*) corresponding to tetrahedral, weakly distorted and highly distorted octahedral sites, all with full occupancy.[13] In both cubic phases reported in this work the lithium sublattice is disordered, but the lithium distribution is considerably different in ncs and cs cubic structures.

According to the present neutron diffraction experiments, in the $Ia\bar{3}d$ sg phase obtained upon exchange at 350 °C lithium occupies the same sites as in the conventional garnets with cubic symmetry and the same sg, i.e. a tetrahedral (24*d*) and a highly distorted split octahedral (96*h*) site.[1] Comparing the occupation of both sites in the exchanged garnet to that of the lithium-rich t-LLZO phase, a clear decrease in the number of Li ions in octahedral sites is observed, meaning that the first Li ions to be exchanged are those in octahedral coordination, which have been found to be more mobile.[9,11] On the other hand, the number of Li ions in tetrahedral sites increases from one in t-LLZO to almost two per formula unit in c350-LLZO. In this respect, the site occupancies follow the same trend as in the non-protonated cubic garnets, in which the tetrahedral and octahedral occupancies increase and decrease, respectively, as the total amount of lithium per formula decreases.[1]

The change from $I4_1/acd$ to $I\bar{4}3d$ for low-T exchanged compounds is a consequence of insertion of a high number of protons into the lattice substituting for octahedral lithium ions. According to neutron diffraction of the c150-LLZO sample, lithium ions are located only in the tetrahedral cavities, split into two sites, 12*a* and 12*b*, that host 0.51 and 1.36 lithium ions respectively. Regarding the inserted protons, they have shown a preference for the emptied octahedral cavities, forming OH-like bonds with the four oxygen atoms belonging to the tetrahedra around the less occupied 12*a* sites. The presence of these O_4H_4 entities, similar to those found in hydrogarnets, provides a high compositional and thermal stability to low-T exchanged LLZO.

Since in t-LLZO there is only one lithium ion in tetrahedral coordination, compared to almost two in c150-LLZO, going from the $I4_1/acd$ to the $I\bar{4}3d$ unit cell requires the partial occupancy of the 16e tetrahedral sites that are empty in t-LLZO. The reason why tetrahedral sites split into two sites instead of joining to a x24 site, as in $Ia\bar{3}d$ sg, has to be ascribed to the preference of protons for specific sites of the garnet unit cell, so as to form O_4H_4 configurations around the vacant 12*a* sites.

It is interesting to relate the stages of hydration and homogeneity of the exchanged sample with the scale of lithium and proton dynamics as a function of temperature.

Though LLZO is highly sensitive to moisture, exchange is a mobility-limited process. When exchange is produced below 100 °C the low lithium and proton mobilities result in an inhomogeneous mixture of phases with different level of hydration. The difficulty in obtaining a single hydrated phase can be explained by the core-shell mechanism of exchange already proposed to explain the exchange in LaLiTiO perovskites.[20]

According to this mechanism, a layer of exchanged material surrounds the core of non-exchanged t-LLZO, resulting in a gradient of proton content from the surface to the center of the grains. This mechanism also explains the homogeneity of the Raman spectra recorded at different points of otherwise inhomogeneous samples. So, hydration quickly drives t-LLZO to a cubic structure, but reaching a homogeneous phase requires a thermal activation. Heating to about 150°C seems to be enough to homogenize the sample composition.

Due to experimental limitations regarding the densification of the samples, a direct measurement of the ionic conductivity of the protonated compounds has not been attempted. However, Li-ion conduction of c150-LLZO is expected to be diminished due to the low lithium content, the absence of octahedral lithium and the stability of Li and H ordering up to 300 °C (Figure S5). Milder exchanges such as those in c350-LLZO, where octahedral Li is still present, might be less detrimental. It is worth to note that dynamic exchange between octahedral and tetrahedral Li sites has been observed in those less protonated compounds[9], although their long range conduction has not been evaluated. However, from the applicability of LLZO point of view, it should be taken into account that aiming the homogeneity of the materials we have used in their preparation extreme conditions far from those present in a real system (powdered samples, maximized exchange rates).

SUMMARY AND CONCLUSIONS

By performing proton for lithium exchange of tetragonal LLZO in a wide range of experimental conditions, we have been able to propose a landscape of phases formed as a function of exchange temperature and proton content. XRD and Raman spectroscopy are used throughout this work for phase identification. Selected compositions representative of the different phases have been analyzed by neutron powder diffraction, which has allowed the study of lithium and proton distribution within the garnet structure.

We have proved that two different cubic phases derive from t-LLZO through proton for lithium exchange. The first one has a non centrosymmetric $I\bar{4}3d$ structure, the second one is a centrosymmetric $Ia\bar{3}d$ phase. The ncs phase can be reached by hydration at low temperature (up to 150 °C) but stabilizing the cs phase at RT requires annealing at higher temperatures (≥300°C).

We have shown that the lithium distribution is quite different in ncs and cs phases. Whereas in the cs phase Li occupies the same octahedral and tetrahedral sites as in the usual cubic phase of lithium conducting garnets, in the most hydrated ncs phase most of the octahedral lithium ions are substituted by protons and tetrahedral sites are split into two sites with half multiplicity, one of them being much more populated than the other. The splitting of the tetrahedral sites as well as the preferential location of protons around the less occupied tetrahedral site in the form of O_4H_4 entities result in the loss of inversion symmetry.

The main factors determining whether the centrosymmetric or the non-centrosymmetric structure forms upon protonation are the temperature at which exchange is performed (linked to lithium dynamics) and the total proton content. Unfortunately, it has been shown that both factors are not independent: the high proton content obtained at low temperature favors the ordering of protons around the vacant tetrahedra while low proton content and higher Li (and proton) mobility at 350 °C lead to a disordered configuration of both Li and H ions.

The deeply hydrated garnets derived from t-LLZO are stable up to at least 300 °C and also upon ageing at RT, in agreement with the excellent stability found by Ma et al. for proton exchanged c-LLZO.[11]

ASSOCIATED CONTENT

Supporting Information Available: Thermogravimetric Analysis data of the manuscript compounds, XRD and Raman data of intermediate (no single phase) phases, study of the thermal evolution by XRD and Raman.

AUTHOR INFORMATION

Corresponding Author

* Alodia Orera, aorera@unizar.es

Funding Sources

This work has been supported by the Spanish Ministerio de Economía and Feder funds through grant MAT2010-19837-C06-06. We are grateful to the Institut Laue Langevin for the neutron beam-time allocated DOI:10.5291/ILL-DATA.5-21-1093.

ACKNOWLEDGMENT

This work has been supported by the Spanish Ministerio de Economía and Feder funds through grant MAT2010-19837-C06-06. A. Orera and G.Larraz acknowledge the financial support provided by the Spanish Ministerio de Ciencia e Innovación through a Juan de la Cierva contract and by Gobierno de Aragón through a PhD grant (B108/11) respectively. The authors wish to thank Servicio General de Apoyo a la Investigación-SAI (Universidad de Zaragoza) and CAI DRX (U. Complutense, Madrid) for technical support in XRD experiments. We are grateful to the Institut Laue Langevin for the neutron beam-time allocated DOI:10.5291/ILL-DATA.5-21-1093.

REFERENCES

(1) Cussen, E. J., *J. Mater. Chem.* **2010,** *20*, 5167-5173.
(2) Thangadurai, V.; Narayanan, S.; Pinzaru, D., *Chem. Soc. Rev.* **2014,** *43*, 4714-4727.
(3) Truong, L.; Colter, J.; Thangadurai, V., *Solid State Ionics* **2013,** *247*, 1-7.
(4) Truong, L.; Howard, M.; Clemens, O.; Knight, K. S.; Slater, P. R.; Thangadurai, V., *J. Mater. Chem. A* **2013,** *1*, 13469-13475.
(5) Galven, C.; Dittmer, J.; Suard, E.; Le Berre, F.; Crosnier-Lopez, M.-P., *Chem. Mater.* **2012,** *24*, 3335-3345.
(6) Galven, C.; Suard, E.; Mounier, D.; Crosnier-Lopez, M.-P.; Le Berre, F., *J. Mater. Res.* **2013,** *28*, 2147-2153.
(7) Gam, F.; Galven, C.; Bulou, A.; Le Berre, F.; Crosnier-Lopez, M.-P., *Inorg. Chem.* **2014,** *53*, 931-934.
(8) Larraz, G.; Orera, A.; Sanjuan, M. L., *J. Mater. Chem. A* **2013,** *1*, 11419-11428.
(9) Larraz, G.; Orera, A.; Sanz, J.; Sobrados, I.; Diez-Gomez, V.; Sanjuan, M. L., *J. Mater. Chem. A* **2015,** *3*, 5683-5691.
(10) Wang, Y.; Lai, W., *J. Power Sources* **2015,** *275*, 612-620.
(11) Ma, C.; Rangasamy, E.; Liang, C.; Sakamoto, J.; More, K. L.; Chi, M., *Angew. Chem., Int. Ed.* **2015,** *54*, 129-133.
(12) Narayanan, S.; Ramezanipour, F.; Thangadurai, V., *Inorg. Chem.* **2015,** *54*, 6968-6977.
(13) Awaka, J.; Kijima, N.; Hayakawa, H.; Akimoto, J., *J. Solid State Chem.* **2009,** *182*.
(14) Rodriguez-Carvajal, J., *Physica B* **1993,** *192*, 55-69.
(15) Momma, K.; Izumi, F., *J. Appl. Crystallogr.* **2011,** *44*, 1272-1276.
(16) Cheng, L.; Wu, C. H.; Jarry, A.; Chen, W.; Ye, Y.; Zhu, J.; Kostecki, R.; Persson, K.; Guo, J.; Salmeron, M.; Chen, G.; Doeff, M., *ACS Appl. Mater. Interfaces* **2015,** *7*, 17649-17655.
(17) Slater, P. R.; Greaves, C., *Solid State Ionics* **1992,** *53*, 989-992.
(18) Kolesov, B. A.; Geiger, C. A., *Am. Mineral.* **2005,** *90*, 1335-1341.
(19) Chakoumakos, B. C.; Lager, G. A.; Fernandezbaca, J. A., *Acta Crystallogr., Sect. C: Cryst. Struct. Commun.* **1992,** *48*, 414-419.
(20) Boulant, A.; Bardeau, J. F.; Jouanneaux, A.; Emery, J.; Buzare, J.-Y.; Bohnke, O., *Dalton Trans.* **2010,** *39*, 3968-3975.

FOR TABLE OF CONTENTS ONLY

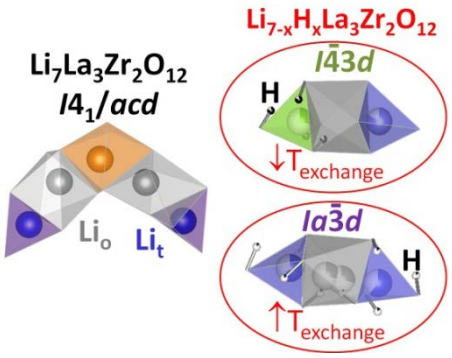

We address the different structural changes undergone by $Li_7La_3Zr_2O_{12}$ as a result of H^+/Li^+ exchange as a function of the proton content and atomic distribution. Deep hydration yields a non centrosymmetric $I\bar{4}3d$ phase where the remaining Li ions split into two tetrahedral sites with different occupancies and protons form O_4H_4 entities. Annealing above 300 °C results in a centrosymmetric $Ia\bar{3}d$ phase with lower proton content in which protons occupy a split pseudooctahedral site.